


Search for nonreciprocal magnons in MnPS₃

A. R. Wildes ^{*}*Institut Laue-Langevin, 71 avenue des Martyrs CS 20156, 38042 Grenoble Cedex 9, France*S. Okamoto *Materials Science and Technology Division, Oak Ridge National Laboratory, Oak Ridge, Tennessee 37831, USA*

D. Xiao

Department of Physics, Carnegie Mellon University, Pittsburgh, Pennsylvania 15213, USA

(Received 14 August 2020; revised 16 November 2020; accepted 5 January 2021; published 15 January 2021)

Recent articles have suggested that the quasi-two-dimensional antiferromagnet MnPS₃ may have nonreciprocal magnons, whereby magnons in a Brillouin zone corner at $+\mathbf{q}$ have different energies than those at $-\mathbf{q}$. The magnons along the Brillouin zone boundaries were measured using neutron three-axis spectrometry, paying careful attention to the resolution function, to determine whether such nonreciprocity was present. The data show that, within the resolution, there are no significant differences between the magnons in opposite Brillouin zone corners. The findings are combined with a recently published study of MnPS₃ by neutron resonant spin-echo spectroscopy and discussed within the context of the theories for nonreciprocal magnons.

DOI: [10.1103/PhysRevB.103.024424](https://doi.org/10.1103/PhysRevB.103.024424)

I. INTRODUCTION

MnPS₃ belongs to a family of layered van der Waals compounds that have attracted considerable attention [1–4]. The van der Waals nature of the compounds gives them physicochemical properties that have been studied as possible candidates for optical sensors and battery materials and even cancer treatments [5]. More recently, the ability to delaminate the compounds has been explored and has attracted the attention of the graphene community [6], especially as a number of the members of the family are intrinsically magnetic.

MnPS₃ is one of the magnetic family members. It has a $C2/m$ space group, with the $S = 5/2$ Mn²⁺ ions forming a honeycomb lattice in the ab planes [7]. The compound orders antiferromagnetically below its Néel temperature of ~ 78 K [8,9], adopting a $\mathbf{k} = 0$ collinear structure where each ion is antiferromagnetically coupled to its three nearest neighbors [10]. The moments are almost normal to the ab planes, tilted by $\sim 8^\circ$ towards the a axis [11]. The paramagnetic susceptibility is isotropic, showing that the compound has a Heisenberg-like Hamiltonian.

The possibilities to use magnetic layered compounds in graphene technology requires the understanding of their spin dynamics. A number of theoretical studies have considered the spin dynamics in a collinear antiferromagnet on a honeycomb lattice. The Mermin-Wagner theorem states that an isotropic Heisenberg Hamiltonian will not give rise to long-range magnetic order in two dimensions [12], and extra terms need to be added to the Hamiltonian to stabilize any ordered magnetic structure. Added terms have included dipole-dipole

anisotropy [13], a Dzyaloshinskii-Moriya interaction [14], and a bond-specific anisotropic exchange [15].

These three theories predict nonreciprocal magnons, where magnons at reduced scattering vectors of $\pm\mathbf{q}$ have different energies. The differences are greatest at the Brillouin zone boundaries. Figure 1(a) shows a reciprocal lattice plane for the honeycomb lattice with the Brillouin zone boundaries indicated.

The theories for the dipole-dipole anisotropy and bond-specific exchange predict that the nonreciprocity takes the form of a splitting in the twofold degeneracy of the antiferromagnetic magnons and that the splitting is different at reduced scattering vectors of $\pm\mathbf{q}$. The theories appear to give the same results in zero magnetic field. The splitting is greatest at the corners labeled J and is zero at those labeled N . The mean energies for the magnons, however, are the same at both points.

The theory for the Dzyaloshinskii-Moriya interaction predicts that the magnons stay degenerate, but the dispersion becomes asymmetric about the Γ point with the magnons at J having different energies than those at N . The last theory has particular interest for graphene technology as it may lead to a spin Nernst effect, where magnons with a selected chirality could be excited and driven using a temperature gradient [14]. It is worth searching for physical representations of such a system to test the theory, and MnPS₃ was specifically presented as a candidate that may have nonreciprocal magnons [13–15].

Experimental evidence for a magnon Nernst effect in MnPS₃ was recently published in the form of thermoelectric measurements of bulk crystals with deposited platinum electrodes [16]. The evidence was most clearly seen in the temperature dependence of the thermoelectric coefficient of

^{*}wildes@ill.fr

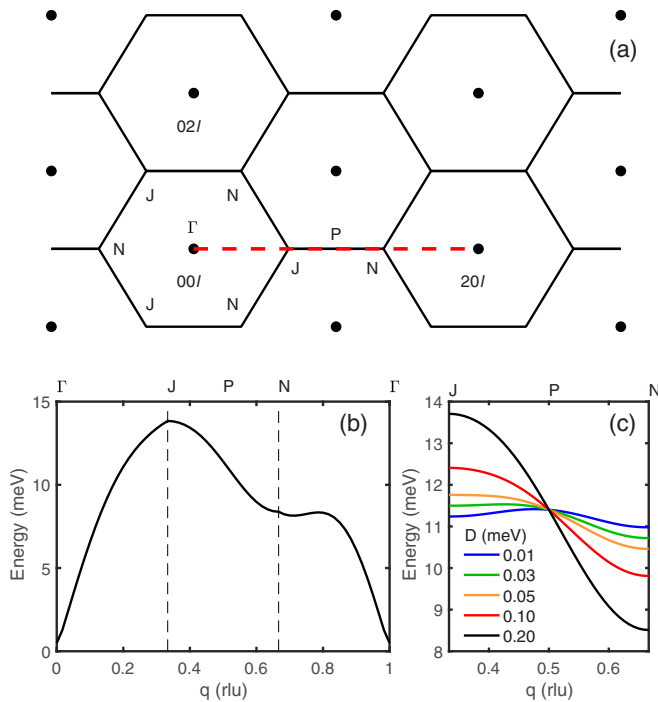


FIG. 1. (a) Schematic showing a plane in reciprocal space for the magnetic structure of MnPS_3 . A Brillouin zone center is marked as Γ , and high-symmetry points on the Brillouin zone boundary are marked with J , N , and P . The sample was mounted in the $h0l$ plane for the experiments, which is orthogonal to the plane shown here. The experiments focused on the scattering along the $h00$ and $h01$ directions, shown by the dashed red line. (b) A calculation for the expected spin-wave dispersion along the dashed red line in (a) for MnPS_3 with a Dzyaloshinskii-Moriya parameter $D = 0.21$ meV, following Ref. [14]. (c) Calculations for the expected spin-wave dispersion along the Brillouin zone boundary of MnPS_3 for different magnitudes of the Dzyaloshinskii-Moriya parameter D .

one of the two electrodes on a sample measured in the absence of a magnetic field. The coefficient changed sign at ≈ 25 K. The authors interpreted this in the context of the theory for the Dzyaloshinskii-Moriya interaction, determining that their data would correspond to MnPS_3 having a Dzyaloshinskii-Moriya parameter D of approximately 0.3 meV.

Such a value for D would result in a large degree of nonreciprocity in the spin-wave dispersion, as shown in Figs. 1(b) and 1(c). Figure 1(b) shows the spin waves along the trajectory marked by the red dashed line in Fig. 1(a) for $D = 0.21$ meV, which is smaller than the value estimated from the thermoelectric measurements. The energies at the J and N points differ by ~ 5.5 meV. Calculations showing the spin-wave dispersion along the Brillouin zone boundary as a function of D are shown in Fig. 1(c). The difference between the spin-wave energies decreases with decreasing D but is still ~ 0.25 meV for $D = 0.01$ meV.

These types of energy differences are readily measurable using neutron scattering techniques. Neutron three-axis spectroscopy is an excellent method for determining the absolute energies of magnetic excitations. The technique was previously used to study the spin dynamics of bulk MnPS_3 [17]. The dispersion surface had an energy gap of 0.5 meV at the

Brillouin zone center and rose to ~ 11.5 meV at the Brillouin zone boundary. The surface was fitted using a Heisenberg Hamiltonian with an easy-axis term for the anisotropy. Satisfactory fits required the inclusion of three in-plane nearest neighbors. The interplanar exchange was $\approx 1/400$ the magnitude of the first nearest-neighbor exchange, showing that bulk MnPS_3 is a good approximation of a two-dimensional magnet. The data suggested that the magnons in MnPS_3 are symmetric on either side of the Brillouin zone center; however, the measurements did not explicitly test for this.

Neutron three-axis spectroscopy easily has sufficient precision to determine whether absolute spin-wave energies at nominally equivalent \mathbf{q} points are the same, but the instrumental resolution broadens the measured width of an excitation peak. Thus, there is a lower limit to the measurable splitting of a peak using this technique, and only one magnon mode was detected in the previous experiments. The technique therefore has limits when trying to measure the type of nonreciprocity predicted from the theories for dipole-dipole anisotropy and bond-specific exchange. Fine splitting can be detected using neutron spin-echo spectroscopy, which is a poor method for determining the absolute energy of an excitation but is excellent for determining the energy difference between two or more excitations in close proximity.

Neutron resonant spin-echo experiments have been performed on MnPS_3 [18]. The data show that the magnons at the N point are degenerate but that they are split by $64 \mu\text{eV}$ at the J point, consistent with the theories for dipole-dipole anisotropy and bond-specific exchange. The measurement could not, however, determine the absolute energies of the two spin waves at either the J or N points and so did not test for nonreciprocity predicted by the Dzyaloshinskii-Moriya theory.

This paper therefore presents a dedicated search for nonreciprocal magnons of the type predicted by the Dzyaloshinskii-Moriya theory [14] using neutron three-axis spectroscopy. The results may be compared with those from the thermoelectric measurements [16] and may be used to put an upper limit on the value of D . Special attention was paid to the instrumental resolution, both as a check to the certainty in the absolute energies of the measured excitations and to verify the small size of the splitting determined in the previous spin-echo measurements [18]. Combined, the data from both the three-axis and spin-echo measurements give a definitive picture for nonreciprocal magnons in MnPS_3 .

II. EXPERIMENT

Neutron three-axis spectroscopy on MnPS_3 was carried out using the IN8 spectrometer at the Institut Laue-Langevin, France [19]. The instrument was configured with a pyrolytic graphite (PG) 002 monochromator and analyzer, which were horizontally flat and vertically focused on the sample. The horizontal divergences were limited using $40'$ collimators before and after both the monochromator and the analyzer. The final wave number was fixed at $k_f = 2.662 \text{ \AA}^{-1}$, and higher-order wavelength contamination was suppressed using a PG filter between the sample and analyzer. The same MnPS_3 crystal used in previous neutron studies [11, 17, 18, 20] was aligned

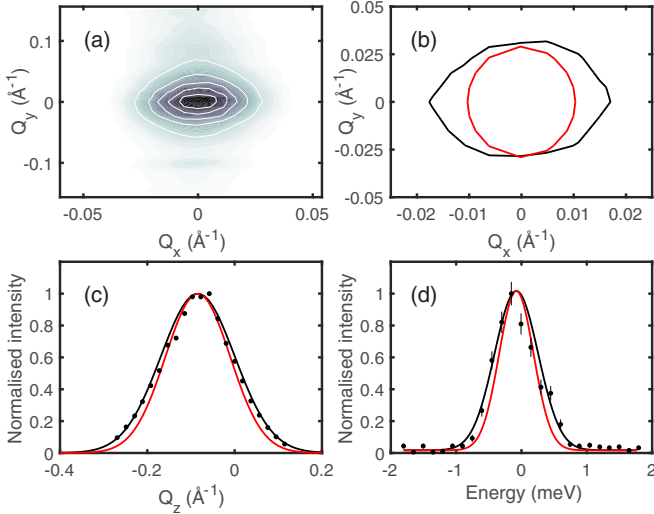


FIG. 2. Measured and simulated resolution at the 200 position. (a) Reciprocal space map of the 200 Bragg peak in the $(h0l)$ plane, with Q_x and Q_y being, respectively, parallel and perpendicular to \mathbf{Q} . (b) Comparison of the FWHM contour for the measured Bragg peak (black) with the calculated resolution (red). (c) Measured width of the 200 Bragg peak along Q_z , which is normal to the $(h0l)$ plane, i.e., along $0k0$. The fit to the data (black line) and the calculated width (red line) are also shown. (d) Measured energy width of the incoherent scattering at a Q equivalent to the 200 Bragg peak. The fit to the data (black line) and the calculated width (red line) are also shown.

such that $(h0l)$ was the scattering plane, and the sample was cooled to 1.8 K using a liquid helium cryostat.

Careful attention was paid to the resolution function of the instrument. An experimental estimate for the \mathbf{Q} resolution, where \mathbf{Q} is the scattering vector, was determined by mapping reciprocal space around the 200 Bragg peak at 1.8 K. This peak arises from purely nuclear scattering as the magnetic structure factor is zero at this position. An estimate of the energy resolution for elastic scattering was determined at a position where only incoherent scattering is expected, corresponding to a rotation from the 200 peak by 15° about the normal to the scattering plane. The resolution was then calculated using the Popovici method [21] in the RESCAL5 library for MATLAB [22].

The data are shown in Fig. 2, along with the estimates from the calculation, with \mathbf{Q} given in reciprocal angstroms. An orthogonal basis is defined such that Q_x is parallel to \mathbf{Q} , Q_y is perpendicular to \mathbf{Q} and in the scattering plane, and Q_z is normal to the scattering plane. Figure 2(a) shows a reciprocal space map of the 200 Bragg peak in the $(h0l)$ scattering plane. The data show that the crystal is not perfect, with the mosaic spread and stacking faults giving rise to a ridge of intensity along Q_y , which is parallel to the \mathbf{c}^* direction at 200. Figure 2(b) shows the FWHM contour for the measured peak along with the FWHM for the calculated resolution. The instrument and measurement parameters for the calculated resolution were all correct and unadjusted for IN8, and the calculation used a mosaic spread of $90'$ for the sample. The comparison is satisfactory in Q_y , but is slightly too small along Q_x . The disagreement is not expected to be important at the

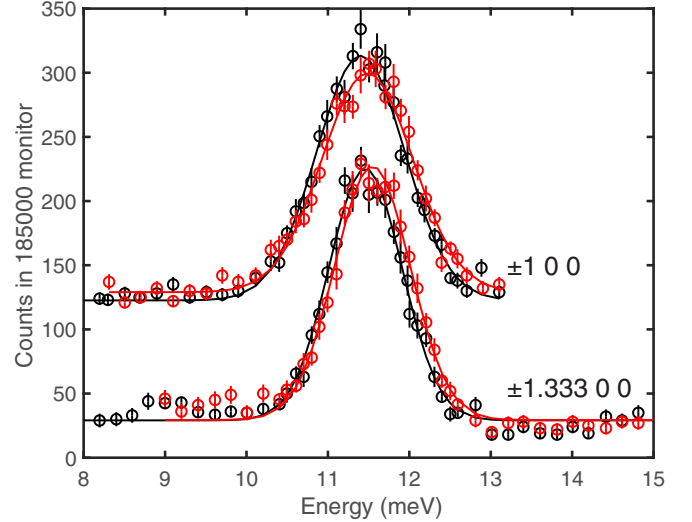


FIG. 3. Data measured at $\pm\frac{4}{3}00$, corresponding to the J and N corners of the Brillouin zone, and ± 100 , corresponding to P points. The measurement time for each data point was ~ 330 s. The $+\mathbf{Q}$ and $-\mathbf{Q}$ data points are shown in black and red, respectively. The data at ± 100 have been shifted vertically by 100 for clarity. Fits of Gaussians, including a flat background, to the data are also shown.

Brillouin zone boundaries where the magnons have very little dispersion. Figure 2(c) shows the width of the 200 peak along Q_z , measured by tilting the sample about the y axis. The peak was fitted with a Gaussian, shown as a black line, which agrees well with the calculated profile, shown as a red line.

The incoherent energy width, shown in Fig. 2(d), is of primary importance. The measurement here is analogous to a constant \mathbf{Q} scan on a dispersionless mode at zero energy transfer. The data were fitted with a Gaussian, shown as the black line, while the red line shows the results of the calculation. The FWHMs were 0.79(4) and 0.62 for the fitted and calculated peaks, respectively; thus, the calculation slightly underestimates the width.

The experiments consisted of energy scans at constant \mathbf{Q} , focusing on the magnetic scattering along the $h00$ and $h01$ directions. As indicated by the red dashed line in Fig. 1(a), this trajectory includes a Brillouin zone boundary with access to the J , P , and N points. Figure 1(a) also shows that a J point at scattering vector $+\mathbf{Q}$ is matched by an N point at $-\mathbf{Q}$. The instrumental resolution is a function of the magnitude of the scattering vector Q and the energy transfer $\hbar\omega$. Corresponding J and N points were measured by rotating the sample by 180° about the normal to the scattering plane, thus allowing a direct relative comparison and minimizing potential systematic errors associated with a different resolution. Similar measurements were performed at the P points. A final series of measurements along the $h01$ direction were performed to test for dispersion along the Brillouin zone boundary and to test for spurious scattering.

III. RESULTS

Figure 3 shows data measured at $\pm\frac{4}{3}00$, corresponding to J and N points, and ± 100 , corresponding to P points. The data show clear peaks from magnons that are approximately

TABLE I. Results from fitting Gaussians to the neutron scattering data at different points on the Brillouin zone boundary. The calculated energy resolution for a dispersionless mode at 11.5 meV is 0.9145 meV.

| $ h $ | $ l $ | Centers (meV) | | FWHM (meV) | |
|-------|-------|---------------|--------------|---------------|--------------|
| | | $-\mathbf{Q}$ | \mathbf{Q} | $-\mathbf{Q}$ | \mathbf{Q} |
| 1.333 | 0 | 11.55(1) | 11.46(1) | 1.09(3) | 1.06(3) |
| 1.333 | 1 | 11.62(2) | 11.43(2) | 1.05(6) | 1.09(5) |
| 1 | 0 | 11.49(1) | 11.40(1) | 1.32(4) | 1.28(3) |
| 1 | 1 | 11.43(4) | 11.32(3) | 1.26(9) | 1.24(7) |

dispersionless with energy $\hbar\omega \approx 11.5$ meV, consistent with the previous measurements that showed spin waves with the same energy and with very little dispersion between $0.5 \leq h \leq 1.5$ [17]. The peaks disappeared in measurements above the Néel temperature, verifying their magnetic origin. The data were fitted with Gaussians to give the peak centers and FWHMs, and the fits are shown in Fig. 3. Similar measurements were performed at corresponding points for $l = 1$, and the fit results are summarized in Table I.

An initial inspection of the peak centers at $|h| = \frac{4}{3}$ shows a systematic difference of 0.09 meV between $\pm\mathbf{Q}$. However, this must be tempered by the observation of a similar difference between the centers at $|h| = 1$. The theories all show that the mean energies for the magnons at the P positions should be equivalent [13–15]. Thus, the small energy differences, which are $<9\%$ of the FWHM, are likely to be an experimental artifact, possibly due to the center of mass of the sample being slightly off the central axis of rotation for the spectrometer. It must therefore be concluded that the measurements show no significant difference between the energies of the magnons at the J and N points.

The possibility that the data at $\pm\frac{4}{3}00$ in Fig. 3 contain, in fact, multiple peaks that are not resolvable within the instrument resolution must be considered. The presence of crystallographic and antiferromagnetic domains may cause the scattering at these positions to consist of the magnons at both J and N points, and thus, the experimental data would be a superposition of three peaks for the dipole-dipole and bond-specific theories and two peaks for the Dzyaloshinskii-Moriya theory. The crystal structure of MnPS_3 is monoclinic, but it is very close to being orthorhombic [7], and being layered, it is prone to stacking faults and twinning. The twins have a distinct relationship, corresponding to a rotation by 120° about the \mathbf{c}^* axis [23]. This rotation in itself would not map J points onto N points; however, such a mapping may occur when combined with stacking faults [24]. The antiferromagnetic domains are equivalent to a rotation of the honeycomb lattice by 180° about the normal to the plane which explicitly maps the J points onto the N points. The antiferromagnetic domain population will depend on the way that the sample is cooled. It is possible to drive MnPS_3 into a monodomain state by cooling the sample in crossed electric and magnetic fields [11], but this was not done during the experiment. It is noteworthy that the same sample was shown to be essentially single domain in the neutron spin-echo experiment [17]. The possible influence of domains can be tested by comparing

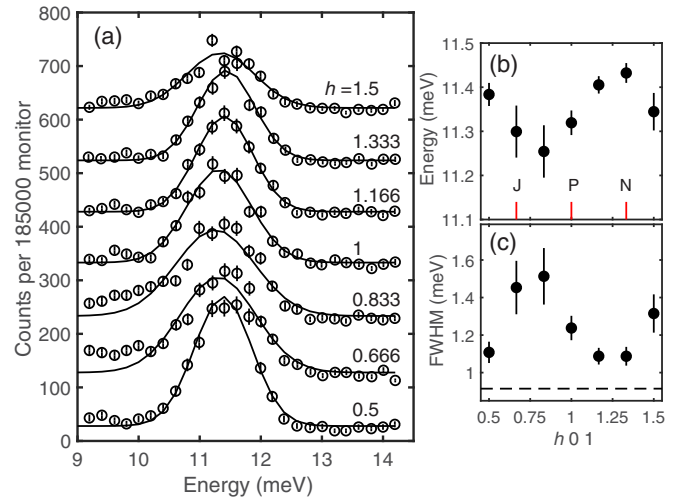


FIG. 4. (a) Measured data along the Brillouin zone boundary along the $h01$ direction, corresponding to the trajectory shown by the red dashed line in Fig. 3. Data at increasing h are shifted vertically by 100 for clarity. Fits of Gaussians, including a flat background, to the data are also shown. (b) The fitted centers of the Gaussians as a function of h . The high-symmetry points along the zone boundary are indicated. (c) The full width at half maximum of the fitted Gaussians as a function of h . The calculated resolution width for a dispersionless mode at 11.5 meV by shown as the dashed line.

the fitted FWHM in Table I with the expected instrumental resolution.

The energy resolution for a dispersionless mode at $\hbar\omega = 11.5$ meV was calculated with the same instrument and mosaic spread parameters used to generate Fig. 2. The calculation at $\hbar\omega = 11.5$ meV gives a FWHM of 0.9145 meV, with the widths being very slightly Q dependent in the fourth decimal place. This may be compared to the fitted FWHM in Table I, which shows that the values at $[\frac{4}{3}0l]$ are larger than the calculation by the same magnitude as those at zero energy transfer. If the difference between fit and calculation is assumed to be systematic, the FWHMs of the peaks at the J and N Brillouin zone corners are resolution limited. It is worth restating that the splitting observed in the neutron spin-echo spectroscopy measurements was $64 \mu\text{eV}$ [18], which is so small as to give a resolution-limited single peak in the three-axis experiment.

Interestingly, a bigger difference is seen at the P position. The magnons at the six P positions are all expected to have the same energy in the Dzyaloshinskii-Moriya theory, and so the widths should be resolution limited [14]. The dipole-dipole and bond-specific models predict a splitting of the magnon degeneracy at these positions, but it is much smaller than that predicted at the J points [13,15]. Furthermore, the spin-echo measurements at this position showed a splitting of $39.4 \mu\text{eV}$ [18], much smaller than the IN8 instrument resolution. The difference may be due to a small amount of spurious scattering on the low-energy side of the peak. Measurements along the $h01$ direction are shown in Fig. 4(a). The data were fitted with Gaussians on a flat background and the fitted centers and FWHM shown in Figs. 4(b) and 4(c), respectively. Some spurious scattering is clearly visible in the lower

energies of the data at $h = \frac{2}{3}$ and $\frac{5}{6}$, causing the fitted centers of these peaks to be smaller and the widths to be broader than the neighbors. Fitting the data with a better estimation of the instrument background, supported by the measurement of spin waves at equivalent points in other Brillouin zones [17], shows that the actual spin-wave energies along this trajectory are practically dispersionless. The peak at 101 may also be very slightly impacted, explaining the slightly broader scattering at this point.

IV. DISCUSSION

The neutron three-axis measurements represent a direct and unambiguous measurement of the absolute energies for the spin waves in MnPS₃. Comparison of the data with the predictions of the Dzyaloshinskii-Moriya model shown in Fig. 1(c) [14] show that, in this compound, D must be substantially less than 0.01 meV. This is at odds with the estimate of $D \approx 0.3$ meV determined from measurements of the temperature dependence of the thermoelectric coefficient [16]. Assuming that the experimental data from the thermoelectric measurements are representative of MnPS₃, the observed Nernst effect must depend upon other processes such as magnon-phonon coupling.

The upper limit for D can be further reduced when considering the neutron resonant spin-echo measurements [18]. As previously stated, a nonzero D does not lift the degeneracy of the magnons. However, an apparent splitting in the Brillouin zone corners might be seen in experiment if the sample had antiferromagnetic domains. The same splitting would then be visible in all Brillouin zone corners as the domains would superimpose the magnons from J and N at the same measured Q . No splitting would be seen at the P points. As shown in Fig. 1(c), the magnon energies at this point are independent of D . These predictions were not seen in the spin-echo measurements, which showed splittings of 64 μeV at the J point, 39 μeV at the P point, and zero at the N point [18]. These results, combined with the neutron three-axis measurements, suggest that MnPS₃ has effectively $D = 0$.

The lack of a Dzyaloshinskii-Moriya interaction is perhaps not surprising in MnPS₃ as it derives largely from exchange interactions with next-nearest neighbors [14,15]. The exchange interactions between these neighbors, determined from neutron spectroscopy [17], is very close to zero, and the superexchange pathways are not straightforward. It is likely that similar effects lead to $D = 0$ in MnPS₃.

The neutron spin-echo results are worth further discussion. When reported [18], they were discussed in the context of the dipole-dipole model [13], which is a logical source of the anisotropy in MnPS₃. A dipole-dipole anisotropy gives rise to both a splitting of the spin-wave energies and a spin-wave gap at the Brillouin zone center. However, the measured splitting and the spin-wave gap were smaller than expected from calculations if dipole-dipole interactions were the sole source of the anisotropy, which would furthermore lead to the moments pointing normal to the ab planes [25] rather than being tilted towards the a axis [11]. The difference was attributed to a single-ion anisotropy which is also believed to be present, based on electron spin-resonance experiments on dilute Mn in CdPS₃ [8]. This anisotropy was determined to

lie in the ab planes, which is consistent with the tilting of the moments and would help to explain the observation that the critical properties of the magnetism in MnPS₃ map onto an XY -like Hamiltonian [20]. The presence of a single-ion anisotropy is somewhat unexpected given that a free Mn²⁺ ion has no orbital angular momentum and its source is not known.

The splitting may also be discussed within the context of the bond-specific exchange model, which gives effectively the same dispersion as the dipole-dipole model in the limit of zero applied magnetic field [15]. This model has two types of anisotropy, one generating a spin-wave gap through an XXZ -type anisotropic exchange and the other lifting the degeneracy of the magnon branches through a bond-dependent exchange modulated by the parameter J^a . The model attributes a nonzero J_a to the presence of toroidal multipoles, and neutron polarimetry experiments show evidence of toroidal moments in MnPS₃ [11]. The moment direction, Z , is defined as being normal to the honeycomb planes, and hence, the model also does not explain the tilted moment axis in MnPS₃. The splitting $\Delta E_{\mathbf{q}}$ is given by the equation

$$\Delta E_{\mathbf{q}} = |J^a| \sqrt{3 + 2 \sum_{n=0,1,2} \cos\left(\mathbf{q} \cdot \boldsymbol{\rho}'_n + \frac{2\pi}{3}\right)}, \quad (1)$$

where $\boldsymbol{\rho}'_0 = [100]$ and $\boldsymbol{\rho}'_{1,2} = [\frac{-1}{2} \frac{\pm 1}{2} 0]$ are next-nearest-neighbor vectors in the monoclinic unit cell. The splitting is therefore $3|J^a|$, $2|J^a|$, and zero at the J , P , and N points, respectively. The ratios for the measured splitting at these points do not quite match those given by Eq. (1), although they are close. Substituting the measured splitting into the equation gives a value for $|J^a| \approx 20 \mu\text{eV}$.

The dipole-dipole anisotropy and the bond-specific exchange models appear to describe the measured spin waves for MnPS₃ in zero magnetic field equally well, although both models fail to describe all the aspects for MnPS₃. The models also make predictions in the presence of an external magnetic field. The bond-specific exchange model was used to calculate the expected spin-wave dispersion for an in-plane magnetic field, predicting a lifting of the degeneracy of the spin waves at the Brillouin zone center. The effects of an in-plane magnetic field in the dipole-dipole model were not explicitly calculated, although calculations of the expected magnetic structure for a field applied normal to the honeycomb planes and parallel to the moment directions were presented, predicting a number of phase changes that were qualitatively verified in MnPS₃ using neutron diffraction and magnetometry [26]. It would be of interest to expand the dipole-dipole calculations to include an in-plane magnetic field and to expand both models to describe the expected critical behavior as a function of temperature and magnetic field and to then compare the predictions for the two models to measurements.

V. CONCLUSIONS

Neutron three-axis spectroscopy was used to search for nonreciprocal magnons in the Brillouin zone corners of MnPS₃. The data show no convincing evidence for nonreciprocal magnons within the precision of the energy

determination of <0.1 meV. When combined with neutron spin-echo measurements, the data suggest that the Dzyaloshinskii-Moriya interaction in MnPS_3 is negligible.

ACKNOWLEDGMENTS

We thank the Institut Laue-Langevin for the allocation of neutron beam time, Dr. A. Piovano and Dr. A. Ivanov for

their assistance with the IN8 instrument, and F. Charpenay and V. Gaignon for technical assistance. A.R.W. thanks Dr. V. Simonet for a critical reading of the manuscript and Dr. T. Ziman for stimulating discussions. S.O. was supported by the U.S. Department of Energy, Office of Science, Basic Energy Sciences, Materials Sciences and Engineering Division. D.X. is supported by AFOSR MURI 2D MAGIC (Grant No. FA9550-19-1-0390).

-
- [1] R. Brec, *Solid State Ionics* **22**, 3 (1986).
 - [2] V. Grasso and L. Silipigni, *Riv. Nuovo Cimento* **25**, 1 (2002).
 - [3] M. A. Susner, M. Chyasnachyus, M. A. McGuire, P. Ganesh, and P. Maksymovych, *Adv. Mater.* **29**, 1602852 (2017).
 - [4] F. Wang, T. A. Shifa, P. Yu, P. He, Y. Liu, F. Wang, Z. Wang, X. Zhan, X. Lou, F. Xia, and J. He, *Adv. Funct. Mater.* **28**, 1802151 (2018).
 - [5] N. Mohamad Latiff, N. F. Rosli, C. C. Mayorga-Martinez, K. Szokolava, Z. Sofer, A. C. Fisher, and M. Pumera, *FlatChem* **18**, 100134 (2019).
 - [6] J. G. Park, *J. Phys.: Condens. Matter* **28**, 301001 (2016).
 - [7] G. Ouvrard, R. Brec, and J. Rouxel, *Mater. Res. Bull.* **20**, 1181 (1985).
 - [8] K. Okuda, K. Kurosawa, S. Saito, M. Honda, Z. Yu, and M. Date, *J. Phys. Soc. Jpn.* **55**, 4456 (1986).
 - [9] P. A. Joy and S. Vasudevan, *Phys. Rev. B* **46**, 5425 (1992).
 - [10] K. Kurosawa, S. Saito, and Y. Yamaguchi, *J. Phys. Soc. Jpn.* **52**, 3919 (1983).
 - [11] E. Ressouche, M. Loire, V. Simonet, R. Ballou, A. Stunault, and A. Wildes, *Phys. Rev. B* **82**, 100408(R) (2010).
 - [12] N. D. Mermin and H. Wagner, *Phys. Rev. Lett.* **17**, 1133 (1966).
 - [13] C. Pich and F. Schwabl, *J. Magn. Magn. Mater.* **148**, 30 (1995).
 - [14] R. Cheng, S. Okamoto, and D. Xiao, *Phys. Rev. Lett.* **117**, 217202 (2016).
 - [15] T. Matsumoto and S. Hayami, *Phys. Rev. B* **101**, 224419 (2020).
 - [16] Y. Shiomi, R. Takashima, and E. Saitoh, *Phys. Rev. B* **96**, 134425 (2017).
 - [17] A. R. Wildes, B. Roessli, B. Lebech, and K. W. Godfrey, *J. Phys.: Condens. Matter* **10**, 6417 (1998).
 - [18] T. J. Hicks, T. Keller, and A. R. Wildes, *J. Magn. Magn. Mater.* **474**, 512 (2019).
 - [19] A. Wildes, K. Anand, and D. Xiao, 2019, <https://doi.ill.fr/10.5291/ILL-DATA.4-01-1607>.
 - [20] A. R. Wildes, H. M. Rønnow, B. Roessli, M. J. Harris, and K. W. Godfrey, *Phys. Rev. B* **74**, 094422 (2006).
 - [21] M. Popovici, *Acta Crystallogr., Sect. A* **31**, 507 (1975).
 - [22] RESLIBCAL, <http://ifit.mccode.org/Applications/ResLibCal/doc/ResLibCal.html>.
 - [23] C. Murayama, M. Okabe, D. Urushihara, T. Asaka, K. Fukuda, M. Isobe, K. Yamamoto, and Y. Matsushita, *J. Appl. Phys.* **120**, 142114 (2016).
 - [24] G. Ouvrard and R. Brec, *Eur. J. Solid State Inorg. Chem.* **27**, 477 (1990).
 - [25] D. J. Goossens, *Eur. Phys. J. B* **78**, 305 (2010).
 - [26] D. J. Goossens, A. R. Wildes, C. Ritter, and T. J. Hicks, *J. Phys.: Condens. Matter* **12**, 1845 (2000).